Front. Optoelectron. 2013, 6(1): 30–45
DOI 10.1007/s12200-012-0298-2

REVIEW ARTICLE

Enabling technologies and challenges for transmission of 400 Gb/s signals in 50 GHz channel grid

Xiang ZHOU (✉)

AT&T Labs–Research, Middletown, NJ 07748, USA

Abstract This paper reviewed the recent progress in transmission of 400 Gb/s, wavelength-division-multiplexed (WDM) channels for optical networks based on the standard 50 GHz grid. We discussed the enabling modulation, coding, and line system technologies, as well as the existing challenges. It is shown that, 400 Gb/s per channel signal can be transmitted on the standard 50 GHz ITU-T grid at 8.4 b/ds/Hz net spectral efficiency (SE) over meaningful transmission reach for regional and metropolitan applications. However, further studies are needed to fully understand the potential for meeting the requirements of long-haul transmission applications.

Keywords modulation, coherent, quadrature amplitude modulation (QAM), fiber, capacity, reconfigurable optical add/drop multiplexer (ROADM), optical filtering, Nyquist pulse shaping

1 Introduction

From a historical point of view, lowering the cost per transmitted bit is the main driving force for the transport interface rate evolution, which was achieved by increasing both the per-channel data rate and the spectral efficiency (SE). So far, the continuing advancement in transport technology has enabled operation at 10, 40, and 100 Gb/s rates within the same optical networks based on the 50 GHz grid. Such a proportional increase of transport interface rate and SE has brought significant cost saving by reducing the transponder foot-print and power consumption and by sharing more capacity over the common network infrastructure. For the next-generation transport system, it would therefore be very attractive to continue to follow this path, i.e., to transmit the 400 Gb/s signals on the standard 50 GHz ITU-T grid, achieving a SE as high as 8 b/s/Hz. Such a high-SE transport system could be compatible with current reconfigurable optical add/drop multiplexer (ROADM) based networks, while providing a 4-fold increase in the transport capacity.

The premise that optical transport costs are decreased most efficiently by increasing both the per-channel data rate and SE has motivated the utilization of high-order quadrature amplitude modulation (QAM) formats, digital coherent detection combined with the use of spectrally-efficient multiplexing schemes, such as orthogonal frequency division multiplexing (OFDM) and Nyquist wavelength-division-multiplexed (WDM) for 400 Gb/s transmission [1–14]. Several of these first demonstrations [3,4,6,8] reported long-haul transmission reaches of 800 to 2000 km, yet the experiments used $>$ 50 GHz WDM channel spacing, which is sub-optimal in terms of maximizing the SE and/or allowing a smooth path for evolving an existing lower-rate system based on the 50 GHz grid.

Experimental demonstration of 400 Gb/s point-to-point transmission on the 50 GHz WDM grid was first achievd in Ref. [9] by using coherent OFDM-32QAM with 80 km transmission reach. The first 400 Gb/s transmission over a 50 GHz-based system with a ROADM was reported in Ref. [10]. In that experiment, eight 450 Gb/s WDM signals based on Nyquist-shaped polarization-division-multiplexed (PDM) 32QAM were transmitted over 4 $\times$ 100 km of ultra-large area fiber (ULAF) and also passed through one standard 50 GHz grid ROADM. In Ref. [11], the transmission distance was improved to 8 $\times$ 100 km by using a broadband optical spectral shaping technique to counteract the ROADM filtering effects. Most recently, it was shown that the transmission distance could be extended to 1200 km by using a time-domain hybrid QAM technique [12]. Without the use of ROADMs (i.e., point to point transmission), more than 3000 km reach has also been demonstrated by using time-domain hybrid 32-64QAM along with improved equalization and phase recovery algorithms [14].

Received October 30, 2012; accepted November 20, 2012

E-mail: zhoux@research.att.com

In this paper, we review recent technology advancements related to 400 Gb/s WDM transmission for 50 GHz grid optical networks. We discuss the enabling technologies and the current challenges. It is showed that the use of time-domain hybrid 32-64QAM, nearly ideal digital Nyquist pulse shaping, distributed compensation for ROADM filtering effects (combined with end-to-end carrier frequency control), distributed Raman amplification, and soft-descion high-gain forward-error-correction (FEC) coding can enable 400 Gb/s transmission on the standard 50 GHz grid over meaningful transmission reach for regional and metropolitan applications.

The remainder of this paper is organized as follows. In Section 2, we describe several key modulation, detection and line systems technologies that could enable 400 Gb/s transmission in optical networks based on the 50 GHz WDM grid. Section 3 is devoted to two 400 Gb/s WDM transmission experiments that included a 50 GHz grid ROADM and were recently demonstrated using the technologies described in Section 2. We present a brief discussion on the remaining challenges and possible solutions to these challenges in Section 4. A comparison of two different 400 Gb/s system design options is also discussed in this section. Finally, we summarize this paper in Section 5.

2 Key enabling technologies

To place 400 Gb/s signals on the standard 50 GHz WDM grid, the system has to tolerate operation at a nominal SE as high as 8 b/s/Hz. However, because the usable bandwidth is actually smaller than 50 GHz due to the well-known channel narrowing caused by cascaded ROADM filtering, an effective SE of greater than 8 b/s/Hz is, in fact, required for a terrestrial system. According to the well-known Shannon capacity theory [15], such a 400 Gb/s system would require more than 11.8 dB higher signal-to-noise ratio (SNR) as compared to a 100 Gb/s system operating at a SE of 2 b/s/Hz, even when using a four dimensional-coded optical modulation format (two orthogonal polarization states plus in-phase and quadrature components of a lightwave) and optimal digital coherent detection. Such a high SNR requirement cannot be met by simply launching more power into the fiber, because the allowable signal power in the fiber is limited by fiber nonlinear effects. Moreover, a higher-SE modulation format is less tolerant to fiber nonlinear effects and implementation imperfections, such as nonzero laser linewidth and limited quantization of digital-to-analog (D/A) and analog-to-digial (A/D) converters [16,17]. To address these significant challenges, SNR-optimized modulation formats, capacity-approaching high-gain FEC, ultra-low noise optical amplification, as well as effective channel bandwidth management, thus become critically important for future 400 Gb/s systems.

2.1 Time-domain hybrid QAM

Higher-order QAM, such as 16, 32 and 64QAM (combined with polarization multiplexing), have recently been experimentally explored to achieve WDM SE's greater than 2 b/s/Hz for WDM systems at 100 Gb/s and higher rates [6,11,13]. However, these regular 2^m-ary QAM systems may not be optimal for a 400 Gb/s system on a 50 GHz grid. In Fig. 1, it is showed the effective required channel bandwidth for regular 2^m-ary QAM formats at several different FEC code rates for a 400GigE system (net data rate = 412.5 Gb/s by taking into consideration the 66b/64b Ethernet line code). Here, the effective channel bandwidth assumes ideal Nyquist signaling with no filtering penalty or inter-symbol interference (ISI). One can see that regular PDM-16QAM, PDM-32QAM, and PDM-64QAM (with 8, 10, and 12 bits/symbol, respectively) allow only certain effective channel bandwidths for a specific FEC code rate.

From Fig. 1, it is apparent that given a certain available effective channel bandwidth, the maximum SE for a particular FEC code rate may not be achievable with the regular PDM 2^m-ary formats. One way to fill these "SE gaps" is to use non-regular QAM formats, such as 36QAM [18]. However, unlike regular QAM formats, which allow multiple binary bits to be mapped/demapped to/from one QAM symbol (i.e., a two dimensional bit-to-symbol mapping problem), a non-regular QAM system requires mapping/demapping multiple binary bits to/from multiple symbols, and is thus more difficult to implement. For the exemplary 36QAM, to fully exploit the available 5.17 bits/symbol SE, one needs to perform mapping of 517 bits to 100 36QAM symbols at the transmitter and demapping of 100 36QAM symbols to 517 binary bits at the receiver. This corresponds to a 200 dimensional bit-to-symbol mapping/de-mapping problem, that is too complex to be implemented in a high-speed optical system.

A better way to realize an arbitrary SE is the recently

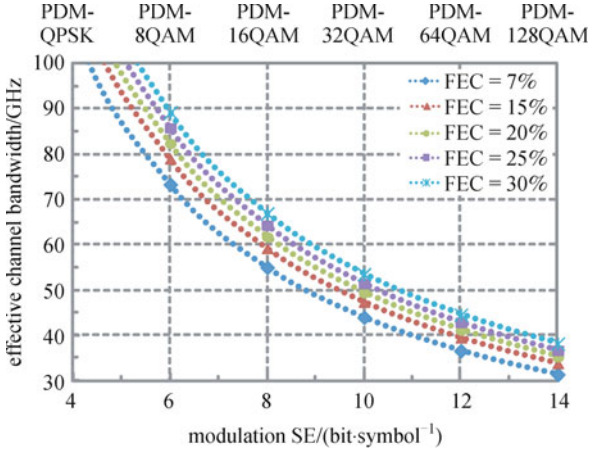

Fig. 1 Effective channel bandwidth versus modualtion SE at several FEC code rates for a 400GigE system

proposed time-domain hybrid QAM technique [12,19]. For this technique, two regular 2^m-ary QAMs with different SE (in terms of bit/symbol) are assigned to different time slots within each time division multiplexing (TDM) frame. Using this method, any SE that falls between the SE of the two regular QAMs can be realized easily by appropriately designing the TDM frame length and the time slot occupancy ratio of the two QAMs. As an example, as shown in Fig. 2, a SE of 5.33 bits/symbol can be implemented by designing a TDM frame length equal to 3 time slots and assigning 32QAM to the first two slots and 64QAM to the final slot. If the Euclidean distance is designed to be identical for both the 32QAM and the 64QAM, such a time-domain hybrid QAM will exhibit a constellation diagram similar to 64QAM but with unequal constellation occupation probability, as can be seen from Fig. 2. For comparison, the constellation diagram for a regular 64QAM is also displayed in Fig. 2.

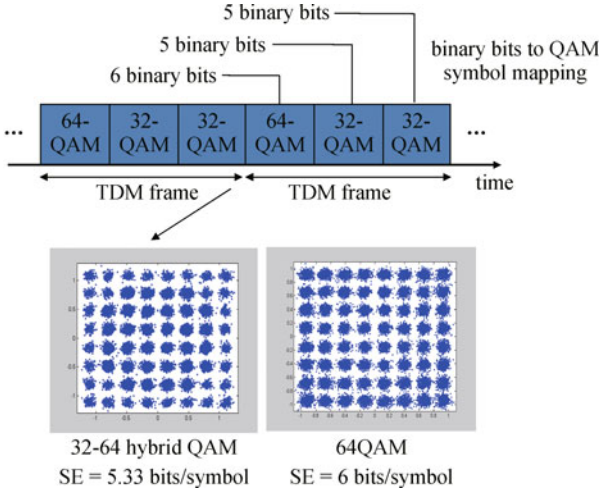

Fig. 2 Exemplary time-domain hybrid 32-64QAM that achieves SE of 5.33 bits/symbol

Arbitrary SE also can be achieved by using frequency-domain based hybrid QAM. For example, one can assign two regular QAMs with different SE to different subcarriers, for an OFDM-modulated system [20]. Compared to such a frequency-domain-based method, time-domain hybrid QAM exhibits several potential advantages such as lower peak-to-average power ratio [21] and better tolerance toward laser phase noise due to the fundamentally shorter symbol period. These two advantages could be important for high-SE optical communication systems, where, in addition to additive Gaussian noise, fiber nonlinear effects and laser phase noise are also major performance limiting factors.

2.2 Nyquist pulse shaping

Nyquist pulse shaping or signaling is another key technology used for several high-SE 400 Gb/s transmission experiments recently reported [10–14]. Nyquist signaling is also known as an orthogonal time-division-multiplexing technique, because although each symbol pulse spreads into many adjacent time slots, no ISI occurs if the sampling is performed at the center of each symbol due to the nature of sinc-shaped pulses, as can be seen from the simulation in Fig. 3(a). Nyquist signaling can achieve the highest SE for any given modulation format, because the spectrum has very sharp rising/falling edges. A square spectrum occupying a bandwidth equal to the baud rate can be achieved by ideal Nyquist signaling with a roll-off factor equal to 0. For any practical Nyquist signaling with nonzero roll-off factor, the signal will occupy an extra-bandwidth equal to the product of the roll-off factor and the signal symbol rate. In Fig. 3(b), the calculated spectrum of a Nyquist signal with a roll-off factor equal to 0.01 is showed. Due to the nearly square spectrum, Nyquist signaling allows multiple WDM channels or multiple sub-channels to be closely packed (to increase WDM SE) without using tight optical filtering. Nearly square spectra also can be generated by using an OFDM-based technique, but an OFDM-modulated signal inherently exhibits a higher peak-to-average power ratio and is also less tolerant to laser phase noise due to the long symbol period.

In Fig. 3(c), we show a simulated eye diagram for a Nyquist-shaped 9 Gb/s baud time-domain 32-64 hybrid QAM signal with a roll off factor equal to 0.01. One can see that a Nyquist-shaped signal has very small eye openings, indicating that it is inherently vulnerable to clock timing errors. But such a problem can be effectively mitigated by using fast digital equalization algorithms that have already been widely adopted in today's digital coherent optical communication systems.

2.3 Distributed compensation of ROADM filtering effects

The non-ideal passband shape of wavelength-selective switches (WSS) can result in significant channel bandwidth narrowing in an optical network using ROADMs to route wavelengths. With recent technological progress in WSS, which is the major filtering component inside a ROADM, the −3 dB bandwidths of up to 45 GHz can be realized for a single ROADM using a single WSS [22]. Even using such state-of-the-art WSS, however, the −3 dB bandwidth will reduce to only 35.7 GHz after passing through 10 cascaded ROADMs.

Narrow optical filtering effects from ROADMS could be a big problem when attempting to transmit 400 Gb/s channels in optical networks based on the 50 GHz grid. Reducing the effective channel bandwidth from 45 to 35 GHz while maintaining the same 400 Gb/s bit-rate requires us to increase the transport SE by about 29%. According to Shanon's theory, this will translate into about 3.8 dB higher SNR requirement, even without considering

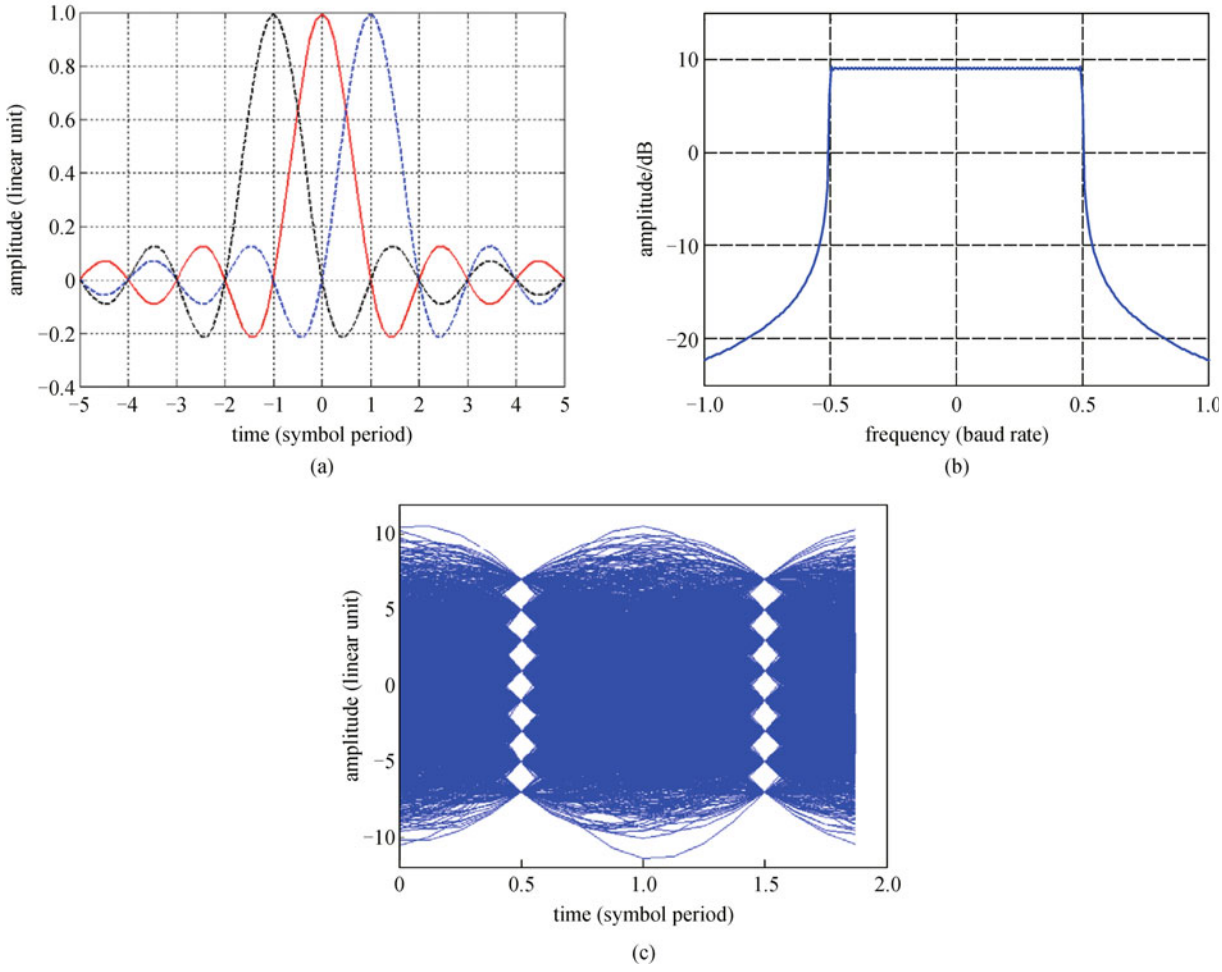

Fig. 3 Simulations of Nyquist pulse signaling. (a) Illustration of three Nyquist pulses in time domain; (b) frequency-domain spectrum with roll-off factor = 0.01; (c) eye diagram of Nyquist-shaped 32-64 hybrid QAM signal

the increased fiber nonlinearity and implementation penalty.

If the filtering effects are not severe, such a bandwidth narrowing problem could be effectively mitigated by the combined use of both pre- and post-transmission digital equalization. However, for the case when an optical signal passes through multiple cascaded ROADMs, the filtering effects can be very strong. For this case, the use of pre-transmission equalization requires a significant increase in the launched signal power, thus causing increased fiber nonlinear impairments. In addition, the use of post-transmission equalization will enhance the noise components (in the high frequency region), further degrading the system performance.

For the general case of significant channel narrowing effects, distributed compensation of ROADM filtering effects [23] could be an effective method to address this challenge. The key idea of this method is to incorporate a broadband optical spectral shaper or an optical equalizer within each ROADM to compensate for the filtering effects from each WSS within that ROADM. In Ref.[11], it is shown that a liquid crystal on silicon (LCoS) based broadband optical spectral shaper could be used as a reconfigurable optical equalizer to compensate for WSS filtering effects. In that experiment, the −3 dB WSS bandwidth was improved from 42 GHz to about 46 GHz. For the case when the WSS passband shape has no (or only weak) dependence on the neighboring channels' add/drop patterns, we propose use of a static optical equalizer based on a simpler Fabry-Perot (F-P) like filter (with a periodic transfer function), as shown in Fig. 4. To illustrate the effectiveness of this method, in Fig. 4(b) we show the simulated power transfer function of an exemplary 50 GHz grid WSS (assuming 5-th order Gaussian passband shape with −3 dB bandwidth equal to 45 GHz) with and without using the F-P-based equalizer. For this specific example, the simulated F-P-based equalizer exhibits a baseband transfer function given by

$$H(f) = 1 + \frac{\alpha}{1 + F \cdot \sin^2\left(\left(\frac{f}{FSR}\right)\pi + \frac{\pi}{2}\right)}, \qquad (1)$$

where F, FSR and α denote the finesse, free spectral range, and the optical coupling parameters, respectively. They are chosen to be 35, 50 GHz and 0.7, accordingly. From Fig. 4(b), one can see that use of the proposed F-P-based equalizer improves the -0.5 dB bandwidth from 37.5 GHz (WSS only) to 44 GHz (WSS + equalizer), without degradation of the channel isolation. Therefore, to enable 400 Gb/s WDM transmission in optical networks based on the 50 GHz grid, we propose this distributed optical equalization method to compensate for the major ROADM filtering effects, and we propose digital pre-and post-transmission equalization to take care of the residual filtering effects.

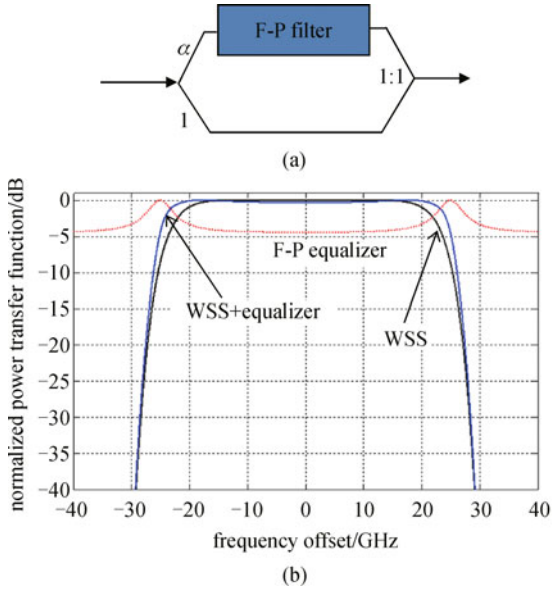

Fig. 4 (a) F-P equalizer (static optical equalizer based on F-P-filter); (b) simulated power transfer functions of F-P equalizer, WSS, and cascade of WSS and F-P equalizer. Details are given in the text and Eq. (1)

2.4 End-to-end carrier frequency control

Offset of the carrier frequency relative to the ITU grid or carrier frequency offset from the center of the ROADM passband is another potential problem for any high-SE WDM system, because such frequency deviation will reduce the usable channel bandwidth, as is illustrated in Fig. 5. According to an Optical Internetworking Forum (OIF) implementation agreement [24], the allowable carrier frequency error from the ITU grid is 2.5 GHz for a 50 GHz-spaced WDM system and 1.25 GHz for a 25 GHz-spaced WDM system. Note that a 2.5 GHz frequency drift could reduce the usable channel bandwidth by 5 GHz, which is 10% of the total 50 GHz channel bandwidth. In addition to transmitter laser frequency error, the actual channel center in a ROADM optical network also may vary over time due to the impact of environmental conditions, such as variation of temperature, humidity,

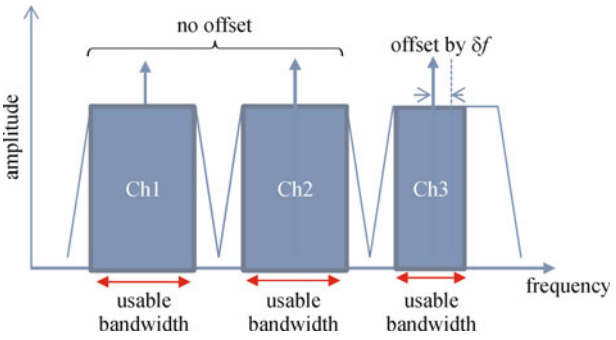

Fig. 5 Impact of carrier frequency drift on usable channel bandwidth

and vibration. Such a ROADM passband variation further decreases channel bandwidth utilization.

One way to address this problem is to tighten the specifications on frequency error of a tunable laser and on the passband stability of a ROADM. But such a method could be costly and difficult to implement. Alternatively, a feedback-based end-to-end carrier frequency control method can be used to mitigate this problem, because the variations of both the laser frequency and ROADM passband typically occur on a significantly slower time-scale than the end-to-end communication time. For this method, some of the receiver performance parameters such as the pre-FEC bit error ratio (BER) are sent back to the transmitter through a supervisory channel, and the frequency of the transmitter laser is then dynamically adjusted based on the received feedback signal until the system achieves the optimal BER performance, which usually occurs when the carrier frequency is tuned to the center of the channel. Such an end-to-end control method could be performed on a channel-by-channel basis, i.e., individual channel optimization; it also may be performed by joint optimization of multiple channels to achieve the lowest average pre-FEC BER of all the considered channels. For the case when the ROADM passband variation is small or passbands of all the WDM channels drift toward the same direction, only individual channel optimization may be needed.

The concept of an end-to-end frequency control method also could be useful for some superchannel systems, where each superchannel consists of multiple independent subcarriers (i.e., subcarriers generated from independent laser sources). The use of the proposed frequency control method could allow a significant reduction of the required frequency guard band (between two neighboring subcarriers) and thus could effectively improve the transport SE.

2.5 High-gain soft-decision FEC and coded modualtion

The continual improvement of FEC coding gain has been one of the major enabling technologies utilized to drive the speed and SE improvement of today's optical transport

systems. The first generation of FEC uses Reed-Solomon (RS) linear block codes represented by RS (255,239), which gives a net coding gain of 5.8 dB with a code rate of 0.93 (7% redundancy). Second generation FEC uses concatenated sets of codes. With the same 7% redundancy and hard decision decoding, > 9.3 dB net coding gain (NCG) has been reported by using continuously interleaved Bose-Chaudhuri-Hocquenghem (CI-BCH) cyclic error correcting code [25]. This is so far the most powerful hard-decision FEC code reported at 7% overhead (only 0.7 dB away from the theoretical limit). The third generation of FEC is based on soft decision and iterative decoding, and the wide adoption of digital coherent detection in 100 Gb/s systems has greatly facilitated the development of soft-decision-based FEC. By using a turbo product code (TPC) with 15% redundancy, 11.1 dB net coding gain has recently been demonstrated in a real-time 120 Gbps coherent polarization multiplexed quadrature phase shift keying (PM-QPSK) MSA transceiver with industry-first integrated analog to digital converter (ADC), digital signal processor (DSP) and soft-decision forward error correction (SD-FEC) in a 40 nm complementary metal–oxide–semiconductor (CMOS) application-specific integrated circuit (ASIC) [26]. With the use of 20% redundancy and low-density parity-check convolution code (LDPC-CCs), a net coding gain of 11.5 dB (with error floor down to 10^{-15}) has been demonstrated using field-programmable gate array (FPGA) emulation [27]. The achieved NGCs for both the 15% TPC and 20% LDPC-CC are 1.1 dB away from Shannon's theory.

Further improvement of FEC coding gain can be achieved by introducing more redundancy as well as joint optimization of modualtion and FEC coding, i.e., the so called coded modualtion. More than 2.5 dB additional NCG is theoretically achievable for a power-constrained binary symmetric additive-white-Gaussian-noise (AWGN) channel by increasing the redundancy from 20% to 150% [28]. For a bandwidth-limited, high-speed, and high-SE optical system (e.g., 400 Gb/s over 50 GHz grid), to keep the same net transport SE, redundancy can only be introduced by increasing constellation size. In accordance with Shannon's theory, to achieve the same net transport SE, increasing the constellation size to accommodate the increased redundancy always helps to improve the performance (i.e., requiring lower SNR). This is because in a AWGN-limited ideal linear system, performance gain obtained from the increase of redundancy through FEC outweighs the SNR penalty paid for the extra modulation SE brought by the increased constellation size [15]. For realistic optical systems, however, one has to consider fiber nonlinear effects and laser phase noise, as well as the limited resolution of D/A and A/D converters. Under realistic considerations, the performance gain from the redundancy may not outweigh the SNR penalty when the constellation size reaches a certain level, because a higher-order modulation format is more vulnerable to all of these extra impairments. Thus, there should exist an optimal FEC code rate (to achieve the longest transmission reach) for a given set of system parameters, such as the net data rate, effective channel bandwidth, laser linewidth, and fiber nonlinear coefficient, as well as the effective number of bits (ENOB) of the D/A and A/D converters. Therefore, in order to operate a transport system with optimal FEC for any given operational condition, a modulation format having the capability to fine-tune the SE is very important, and the previously described time-domain hybrid QAM technique can serve this purpose.

2.6 Distributed Raman amplification

To compensate for the fiber loss, the signal requires amplification after being transmitted over a certain distance (typically 80–100 km in a terrestrial network). So far, discrete erbium-doped fiber amplifiers (EDFA) have been widely deployed in optical links. Although EDFA-only line systems can support 100 Gb/s WDM systems over more than 2000 km reach by using coherent PDM-QPSK and 15%–20% soft-decision FEC [29], the EDFA's relatively high noise figure (~5 dB) could be a disadvantage for future 400 Gb/s systems, particularly for transmission of 400 Gb/s in 50 GHz optical networks. For future 400 Gb/s systems, ultra-low-noise optical amplification techniques, such as distributed Raman amplifiers (DRA), may be required to address the high SNR requirement. Because the gain provided by a DRA is distributed along the fiber link, noise generated from the Raman amplification process is attenuated along with the signal when they propagate down the fiber, resulting in significantly less noise compared to the case of a discrete EDFA, where the noise does not experience any attenuation (within the same span). For a typical WDM system using standard single-mode fiber (SSMF) and 80 km spans, ~5 dB net optical signal noise ratio (OSNR) improvement can be expected by using purely backward Raman amplification compared to using conventional discrete EDFAs. Note that this net OSNR improvement occurs even though the signal power for a Raman system must be reduced to maintain the identical nonlinear phase shift for both systems [30]. Additional performance gain can be achieved by using both forward and backward Raman amplification [12].

In addition to ultra-low-noise optical amplification, new low-loss and low-nonlinearity fiber could also be used to improve the OSNR for some green-field deployments, where there are no existing fibers or where the existing fibers have been exhausted.

3 50 GHz-spaced 400 Gb/s transmission experiments

The feasibility of 400 Gb/s transmission over a 50 GHz-based system with a ROADM has been experimentally

demonstrated using both PDM-32QAM [11] and PDM-hybrid-32-64QAM [12]. For both experiments, close to ideal Nyquist pulse shaping was used to narrow the spectrum and an LCoS-based broadband optical equalizer was used for compensation of ROADM filtering effects. To address the challenge of the high SNR requirement, distributed Raman amplification was employed and the channel bit-rates were high enough to cover the required overhead for the state-of-the-art high coding gain FEC that was assumed. In addition, the carrier frequency of each WDM channel was fine tuned (to the center of the channel) to achieve the optimal performance.

3.1 8 × 100 km using PDM-32QAM [11]

The transmitter used for generating the 450 Gb/s PDM-Nyquist-32QAM signal is shown in Fig. 6. To overcome the limitation of the available D/A converter bandwidth, five 9.2 GHz-spaced subcarriers were used for each channel. The five frequency-locked subcarriers were generated from a single laser source by using two Mach-Zehnder modulators (MZMs), each driven with a 9.2 GHz clock, and followed by either a 12.5/25 GHz interleaver filter (ILF) or two cascaded 25/50 GHz ILFs. The spectra of the generated three odd and two even subcarriers are displayed in Fig. 6 as insets. All unwanted harmonics were suppressed to be at least 33 dB below the subcarrier signals. The odd and even subcarriers were modulated by two independent I/Q data modulators, each driven with a pre-equalized 9 Gb/s baud Nyquist 32-QAM signal with $2^{15}-1$ pseudorandom pattern length. The Nyquist pulse shaping had roll-off factor of 0.01. Frequency-domain based pre-equalization [31] was used to compensate for the band-limiting effects of the D/A converters, which have 3 dB bandwidths < 5 GHz at 10 bit resolution and a 24 GSa/s sample rate. Then the sets of two and three 45 Gb/s sub-carriers were passively combined and polarization multiplexed with ~22 ns relative delay, resulting in a 450 Gb/s signal that occupied a spectral width of 45.8 GHz, sufficiently well confined to be placed on the 50 GHz ITU grid.

The experimental setup for the WDM transmission of 5 × 450 Gb/s PDM-Nyquist-32QAM signals over 800 km and through one 50 GHz grid ROADM is shown in Fig. 7. The five 450 Gb/s, 50 GHz-spaced, C-band channels were derived from odd (192.40 to 192.60 THz) and even (192.45 to 192.55 THz) sets of multiplexed, 100 GHz-spaced external cavity lasers (ECL) with ~ 100 kHz linewidth, which were combined and then modulated by the transmitter of Fig. 6. For this experiment, an LCoS-based dynamic, broadband optical spectral shaper (with 1 GHz resolution) followed by a booster EDFA were inserted

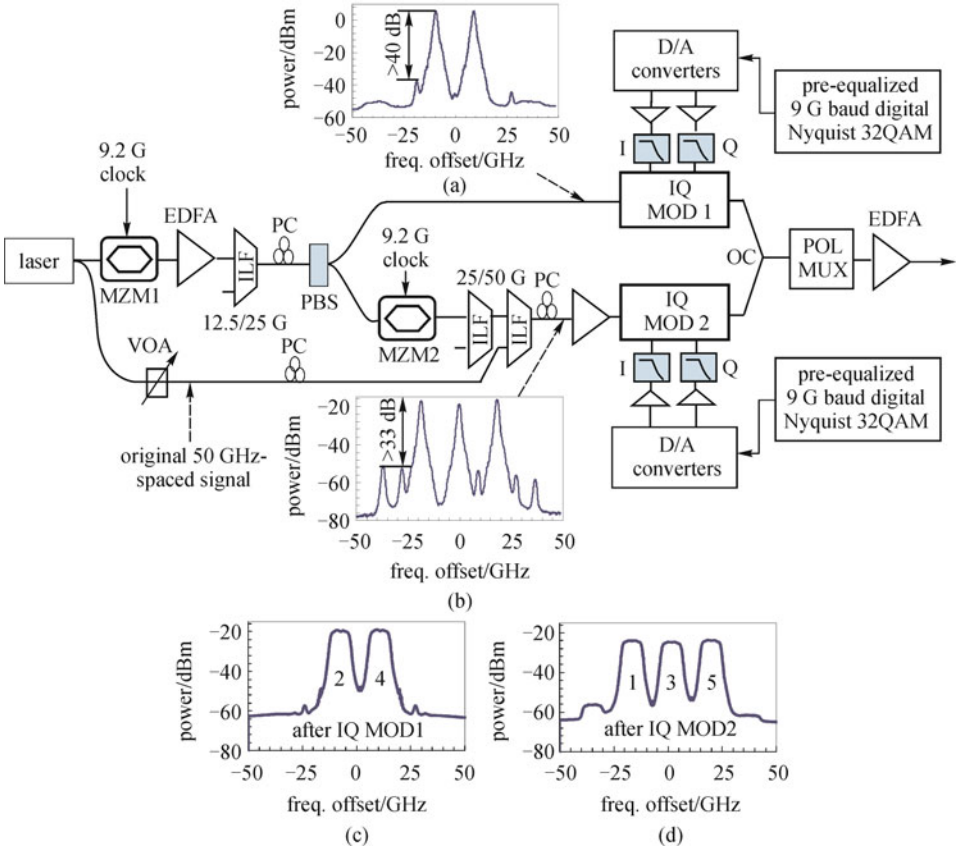

Fig. 6 450 Gb/s PDM-Nyquist-32QAM transmitter. VOA: variable optical attenuator, PC: polarization controller, PBS: polarization beam splitter

before the 50 GHz grid ROADM. This optical spectral shaper was used to pre-compensate the ROADM filtering. The ROADM emulator consisted of a 1 × 8, 50 GHz-spaced WSS based on liquid-crystal technology to emulate the filtering from a ROADM. Odd and even channels were sent to separate WSS output ports, for maximum filtering, and a relative delay of 175 symbols decorrelated the odd and even channels before they were recombined using a 50/100 GHz interleaver. Filtering from the WSS passband was significant, as the −3 and −6 dB bandwidths are 42.2 and 46.6 GHz, respectively. Following the ROADM, the signal was sent into a re-circulating loop, which consisted of four 100-km spans of ultra-large-area (ULA) fiber with, at 1550 nm, average Aeff of 135 μm^2, average attenuation of 0.179 dB/km, and average dispersion of 20.2 ps/nm/km. After splicing the span inputs to standard single-mode fiber jumpers and including a 1450/1550 nm WDM coupler for the counter-propagating Raman pumps at the span outputs, the total span losses were 19.2, 19.6, 19.2, and 18.9 dB. Hybrid Raman-EDFAs were used, with an on-off Raman gain of 11 dB per span from ~1450 nm pumps. After two circulations (800 km), the spectrum of the five 450 Gb/s channels was flat to within 1 dB, for total span input powers ranging from 6 to 12 dBm. The optimal total launch power at the span inputs was 9 dBm.

A DSP-enabled coherent receiver was used for the detection and demodulation of the received PDM-Nyquist-32QAM signal. The polarization- and phase-diverse coherent receiver front-end consisted of a polarization-diverse 90-degree hybrid, a tunable ECL of ~100 kHz linewidth serving as the local oscillator (LO), and four balanced photo-detectors. For our experiments, each subcarrier was independently received by passing the signal through a tunable optical filter with ~37.5 GHz −3 dB bandwidth, and the LO was tuned to be within 200 MHz of the center frequency of each subcarrier. A four-channel real-time sampling scope with 50 GSa/s sample rate and 16 GHz analog bandwidth performed the sampling and digitization (ADC) function, followed by post-transmission DSP of the captured data on a desktop computer. For this experiment, the ADC bandwidth was set to be 9 GHz, which we found to be the optimal electrical bandwidth for a 9 G baud signal.

For the offline DSP, the clock used to resample the signal was extracted by using the "4th-power and filter method" [32], because the popular squaring-type clock recovery circuit does not generate a clock tone for an ideal Nyquist-shaped signal. For the 2 × 2 adaptive equalizer (T/2-spaced, 51 taps), the classic constant-modulus algorithm (CMA) was used in the first stage to achieve pre-convergence, and after the preconvergence was reached, a decision-directed least-mean-square (DD-LMS) algorithm was then used for the steady-state optimization. The frequency offset between the LO and the signal was estimated by using a newly proposed blind frequency search method [31], while the carrier phase was estimated in two stages. First, the carrier phase recovered from the previous symbol was used as an initial test phase angle, and then the "decided" signal made following this initial test phase angle was used as a reference signal for a more accurate ML-based phase recovery through a feed-forward configuration [33]. For the first block of data, the initial

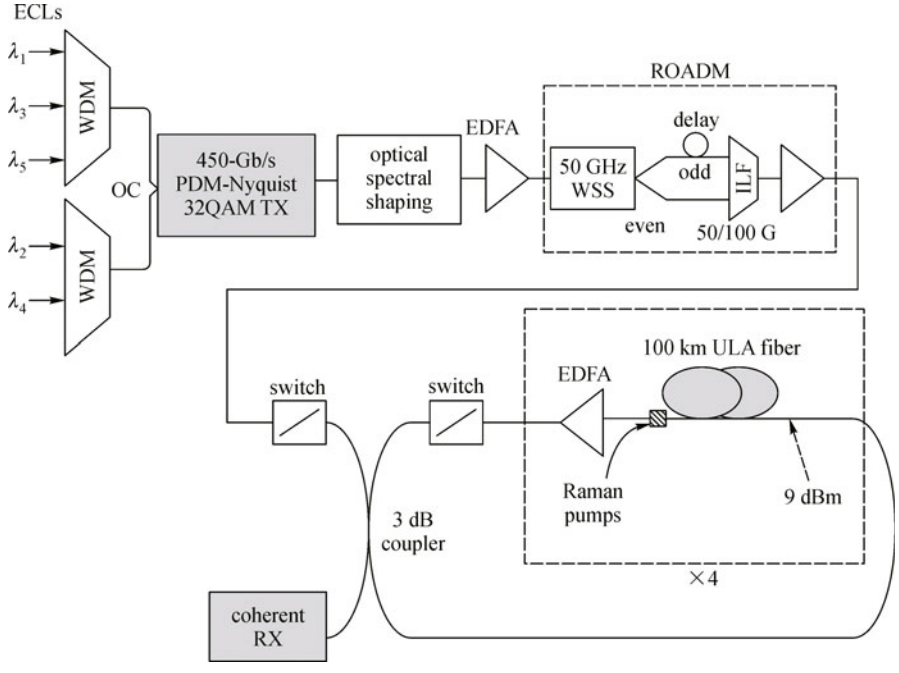

Fig. 7 Set-up for 5 × 450 Gb/s transmission over 800 km. OTF: optical tunable filter. ILF: interleaver filter. OC: optical coupler; PC: polarization controller

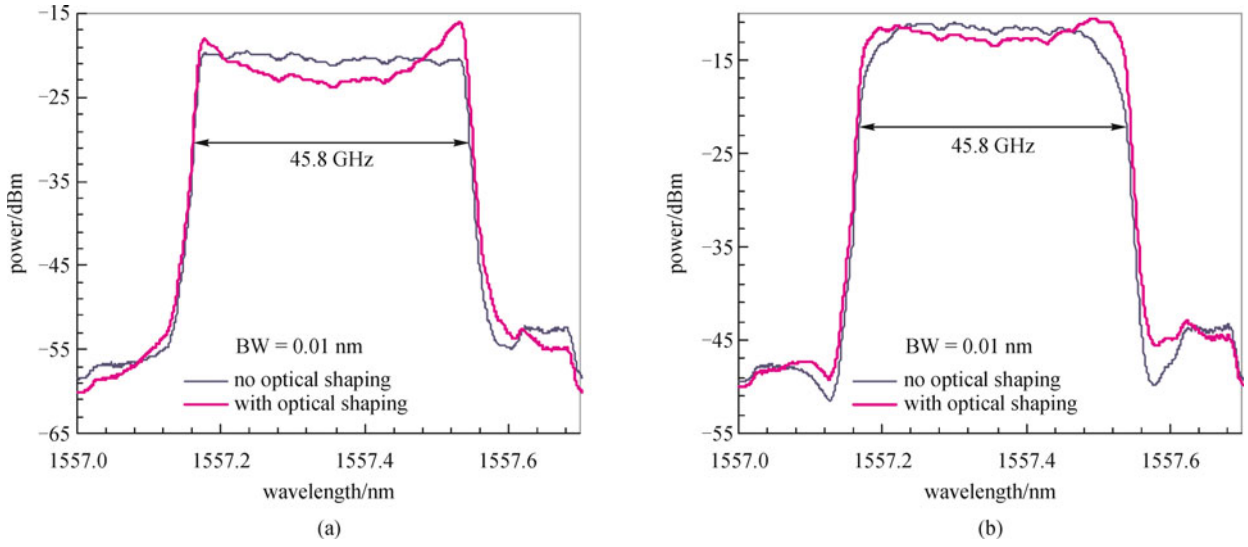

Fig. 8 Measurements of optical spectra for single channel with (thick) and without (thin) optical spectral shaping (a) before ROADM and (b) after ROADM

phase angle was obtained by using the blind phase search (BPS) method [17]. To reduce the probability of cycle slipping (no differential coding/encoding was used in this experiment), a sliding-window-based symbol-by-symbol phase estimation was employed. For BER calculations, errors were counted over more than 1.2×10^6 bits of information. The standard Gray coding based symbol-to-bit mapping technique was used to minimize bit error ratio.

In Figs. 8(a) and 8(b), we show the measured optical spectra of a single 450 Gb/s, 32QAM channel before and after the 50 GHz ROADM, respectively. The thin lines show the spectra without optical spectral shaping. It is clear that when the signal (without optical spectral shaping) passed through the 50 GHz ROADM, significant filtering occurred. The power loss due to this filtering effect could be largely pre-compensated by using broadband optical spectral shaping, as shown by the thick lines in Figs. 8(a) and 8(b). Using this spectral shaping, the measured optical spectra of the five 450 Gb/s dense wavelength division multiplexing (DWDM) signals prior to and after the ROADM are shown in Figs. 9(a) and 9(b), respectively. The filtering effects of all the five channels were largely pre-compensated.

Figure 10 shows the measured OSNR sensitivity for a 450 Gb/s PDM-Nyquist-32QAM signal (the average of the five subcarriers) for three different scenarios: a single channel without optical filtering from the ROADM (i.e., the back-to-back case, no optical shaping applied), with filtering from the ROADM when the optical spectral shaping was applied, and finally with filtering from the ROADM but without optical spectral shaping. For comparison, a theoretical OSNR sensitivity curve is also displayed in Fig. 10. The recovered Nyquist-32QAM constellation diagram at an OSNR of 37 dB for a single 450 Gb/s channel also is shown in this figure. Without

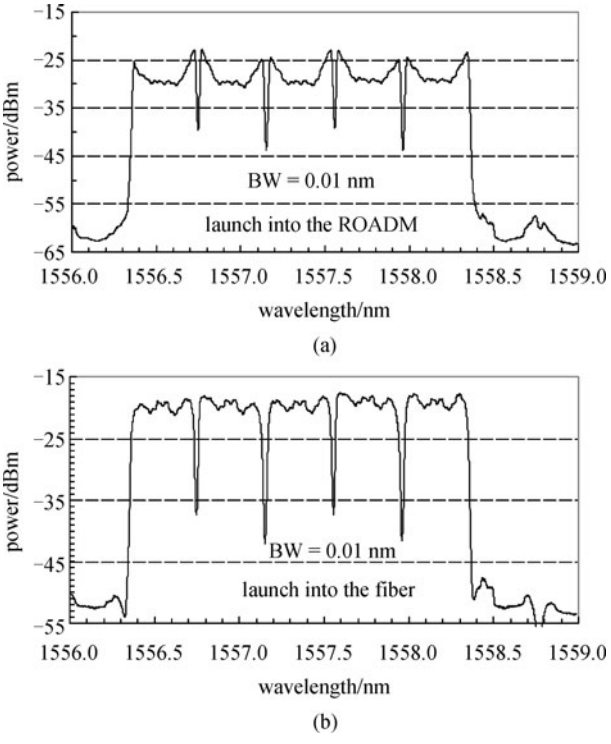

Fig. 9 Measurements of optical spectra of the five DWDM signals with optical spectral shaping (a) before ROADM and (b) after ROADM at the fiber launch

ROADM filtering, 26.8 dB OSNR is required to achieve 4.5×10^{-3} BER (the threshold for a 7%-overhead FEC [25]), which is 3.2 dB away from the theory. In the presence of ROADM filtering, one can see that the use of optical spectral shaping improved the OSNR sensitivity by more than 1.6 dB at 4.5×10^{-3} BER. At 4.5×10^{-3} BER, the measured OSNR penalties from inter-subcarrier and

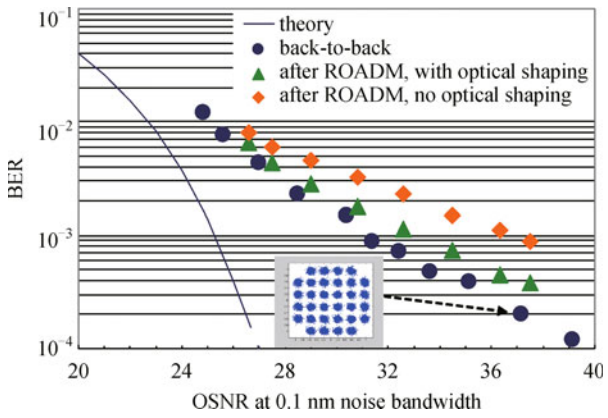

Fig. 10 OSNR sensitivity for 450 Gb/s PDM-Nyquist-32QAM signal

inter-WDM channel are smaller than 0.8 and 0.1 dB, respectively (details can be found in Ref. [23]).

The measured BER of all five WDM channels after 800 km transmission, at the optimal total launch power of 9 dBm (2 dBm/ch) is presented in Fig. 11, where the BERs shown are the average over the five subcarriers of each WDM channel. The inset shows the measured BER for the center channel located at 192.5 THz as the total launch power into the spans was varied. The received OSNR was approximately 31 dB/0.1 nm at 9 dBm total launch power. At the optimal launch power, the BER performance of the five individual subcarriers is also displayed in the inset. The BER of all five channels was better than 3.8×10^{-3}, and the worst subcarrier BER was 4.3×10^{-3}, both of which are lower than the BER threshold for a 7% continuously interleaved BCH code (4.5×10^{-3} [25]).

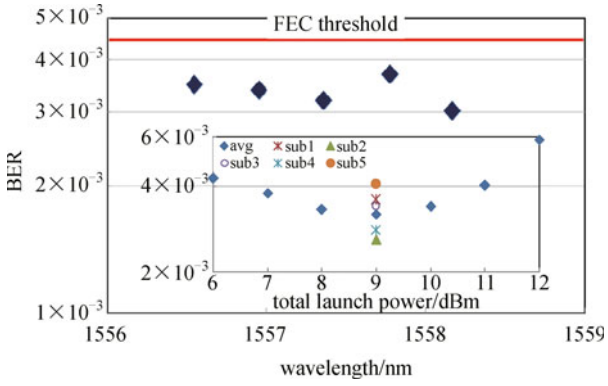

Fig. 11 Measured BER of five 450 Gb/s DWDM channels after 800 km transmission. The inset displays the measured BER for the center DWDM channel versus total launch power for all five 450 Gb/s channels

3.2 12 × 100 km using PDM-32-64 hybrid QAM [12]

As discussed in Section 2.4, high-gain soft-decision FEC is an important enabling technology for high SE at 400 Gb/s, and the constellation size can be increased to accommodate increased redundancy. To allow use of soft-decision FEC having 20% overhead, higher-order hybrid 32-64QAM was used in a second 400 Gb/s WDM transmission experiment with 50 GHz channel spacing. Figure 12 shows the transmitter setup. Similar to the experiment described in the previous sub-section, five 9.2 GHz-spaced and frequency-locked subcarriers were used to create the required 504 Gb/s signal (including the 20% soft-decision FEC and 2.18% training overhead). For this experiment, the unwanted harmonics were suppressed to be 35 dB lower than the subcarrier signals. The two even subcarriers were modulated with a pre-equalized 9 G baud Nyquist 64-QAM signal with 2^{15} pseudorandom pattern length. The Nyquist pulse shaping had roll-off factor of 0.01. Digital pre-equalization was used for compensation of band-limiting effects caused by the digital-to-analog (D/A) converters, which have 3 dB bandwidths < 5 GHz at 10 bit resolution and 24 GSa/s sampling rate. 24 GSa/s over-sampling (combined with the use of four 4.9 GHz low-pass electrical filters) was employed in this experiment to suppress the DAC aliasing components (to reduce inter-subcarrier crosstalk). The odd subcarriers were modulated by a pre-equalized 9 G baud Nyquist 32-64 time-domain hybrid QAM signal having a length of 10923 TDM frames, where each TDM frame consists of three symbols: the first symbol is 64QAM and next two symbols are 32QAM. The total pseudorandom pattern length is then $3 \times 10923 = 2^{15} + 1$. And the aggregate SE is 5.33335 bits/symbol. For ease of processing, the Euclidean distance for the 64QAM and 32QAM are designed to be identical, resulting in a 64QAM-like constellation with un-equal constellation occupation probability, as can be seen in Fig. 2. Such an "equal-distance" design enables blind equalization before TDM synchronization. For simplicity, the powers of the five subcarriers were adjusted to be equal at the input to the polarization multiplexer. The main purpose of using different modulation formats for the odd and even subcarriers is to verify that a time-domain hybrid 32-64QAM is more tolerant to implementation imperfections than the standard 64QAM.

The WDM transmission setup is similar to the one shown in Fig. 7. The five 504 Gb/s, 50 GHz-spaced, C-band channels are still derived from odd (192.40 to 192.60 THz) and even (192.45 to 192.55 THz) sets of multiplexed, 100 GHz-spaced ECL with ~100 kHz linewidth. After the polarization multiplexer, booster amplifier, and optical spectral shaper, the signals entered the recirculating loop. For this experiment, however, all Raman amplification was used in each span: counter-pumps at 1435 and 1455 nm with 310 and 650 mW, respectively, provided an average of 17 dB on-off Raman gain, while co-pumps at 1455 nm with 180 mW provided an average of 3 dB on-off gain. In addition, a loop-synchronous polarization controller was added after the last span, which was then followed by a gain-flattened EDFA to compensate the loss of the loop

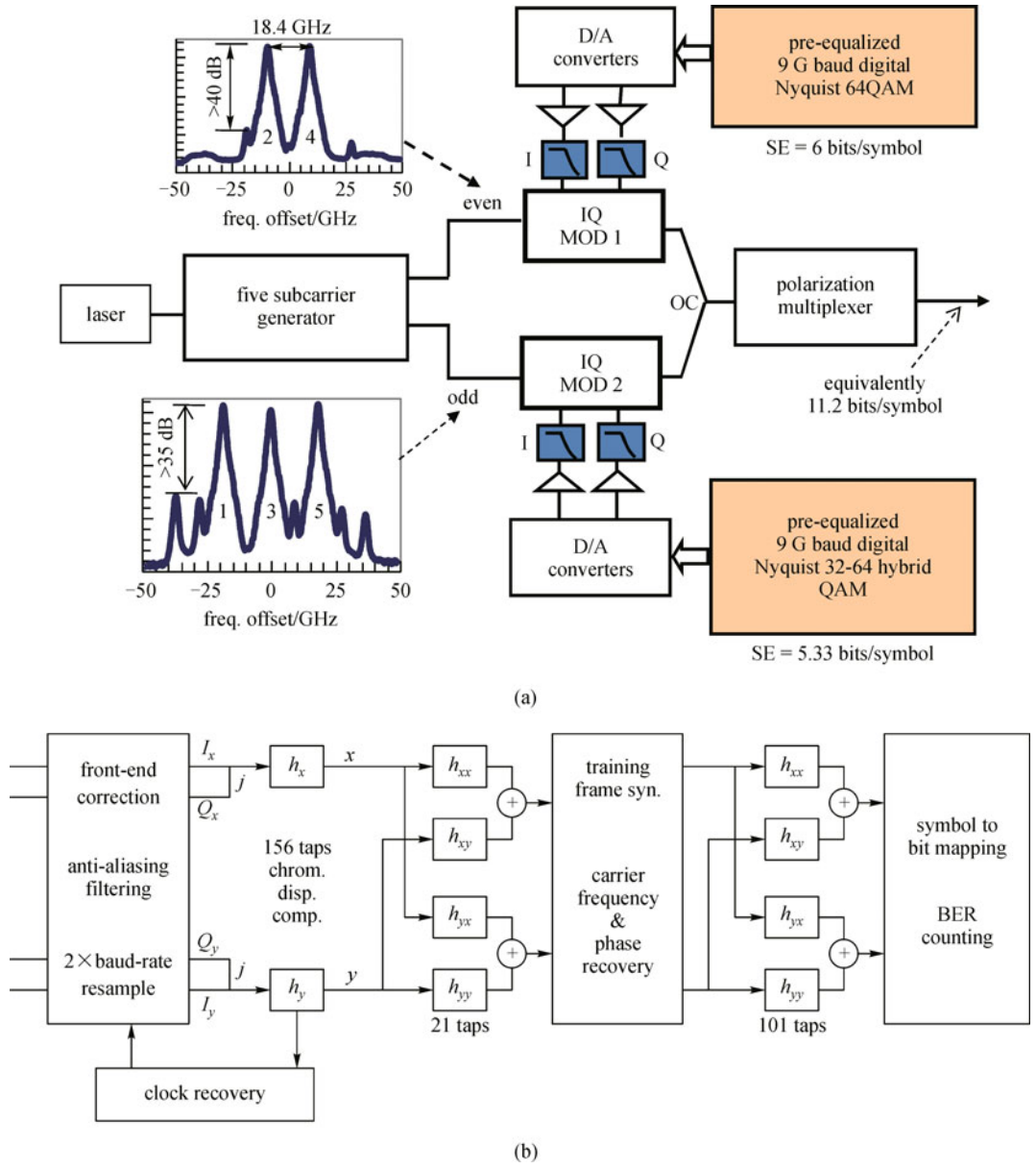

Fig. 12 (a) 504 Gb/s PDM-32-64 hybrid QAM transmitter; (b) offline DSP functional block daigram

components. After three circulations (1200 km), the spectrum of the five 504 Gb/s channels was flat to within ~1.5 dB, and the measured OSNR of the five WDM channels was 30.9 dB/nm on average at 6.5 dBm total launch power.

After 1200 km transmission, each subcarrier was independently received with the polarization- and phase-diverse coherent receiver and offline DSP of the captured data, as described in the previous subsection. Two-stage adaptive equalization was used in the offline processing: first a constant modulus algorithm (CMA)-based blind equalizer (2 × 2, 21-tap and T/2-spaced) was used to perform an initial equalization and then a training-based equalizer (101-tap and T/2-spaced) was used for further optimization. We have found that imperfect phase recovery is a significant problem for achieving the optimal equalization performance. The use of training signals allows better phase recovery (for the training signals), and therefore the equalizer is more likely to converge to the optimal point. For this experiment, the first 293 symbols of every 16384 symbols were used to train the equalizer. This training sequence was also used for carrier-LO frequency offset estimation, following the CMA equalization. Note that TDM and pattern synchronization were achieved by doing correlation analysis of the CMA-equalized signal. Phase recovery was performed following frequency recovery by using a two-stage method described in the previous subsection. To mitigate the impact of phase-error

propagation (and cyclic phase slipping), the first 4 symbols of every 1024 symbols were used as training symbols for an absolute phase check (no differential coding was used in this experiment). The total overhead for the equalizer and phase check was 2.18%. For BER calculations, errors were counted over 1.2×10^6 bits of information for each subcarrier (6×10^6 bits for each channel).

In Figs. 13(a) and 13(b), we show the measured back-to-back performance (average of the five subcarriers) of a single 504 Gb/s, PDM 32/64-hybrid QAM channel; the spectrum before optical spectral shaping is shown in the inset. The required OSNR at 2.4×10^{-2} BER (a 20% soft decision FEC threshold [34]) was 25 dB, which is 2.5 dB higher than the theoretical required OSNR. However, at the same baud rate and net SE and with the same transmitter hardware, PDM-32QAM requires 26.8 dB OSNR to achieve the 7% FEC hard decision threshold 4.5×10^{-3} [25]. Thus, the use of hybrid 32-64QAM and 20% soft decision FEC improves the OSNR sensitivity by 1.8 dB. The BER performance for each of the five subcarriers is shown in Fig. 13(b). The advantage of the PDM 32-64 hybrid QAM subcarriers over the PDM 64-QAM subcarriers is clearly evident. Such a significant performance difference arises not only from the fundamental Euclidean distance difference (under identical average power, PDM 32-64 hybrid QAM has larger Euclidean distance than PDM-64QAM, which in theory translates into about 2 dB OSNR sensitivity advantage), but also from the fact that PDM-64QAM is less tolerant to implementation imperfections, such as non-ideal digitization resolution and non-ideal laser linewidth. In addition, 64QAM is also less tolerant to inter-subcarrier crosstalk. At 2×10^{-2} BER, the measured OSNR penalty from inter-subcarrier crosstalk was increased from less than 0.3 dB for hybrid PDM 32-64QAM to 0.9 dB for PDM-64QAM.

Figures 14 to 16 show transmission results after 1200 km. The effects of optical spectral shaping are clearly shown in the launch signal spectrum (Fig. 14 inset). Figure 14 plots the performance of the center WDM channel as a function of the total launch power with only counter-pumping and compares it to the performance with co- and counter-pumping. There was about 0.4 dB Q improvement when using co- and counter-pumped Raman (3 dB co-Raman gain and 17 dB counter-Raman gain), and the optimum launch power was 6.5 dBm (-0.5 dBm per 504 Gb/s channel) with co- and counter-pumping, compared to 8 dBm with only counter-pumping. The measured BER of all five 504 Gb/s WDM channels (i.e., the average of the five subcarriers for each channel) as well as the BER performance of the five individual subcarriers of Ch3 at the optimum total launch power are presented in Fig. 15. The recovered PDM-64QAM and PDM-32-64 hybrid QAM constellation diagrams are displayed in Figs. 16(a) and 16(b), respectively. Although the worst PDM 64-QAM subcarrier had a BER of 2.8×10^{-2}, the BERs of all five WDM channels were better than 1.8×10^{-2} (see Fig. 15),

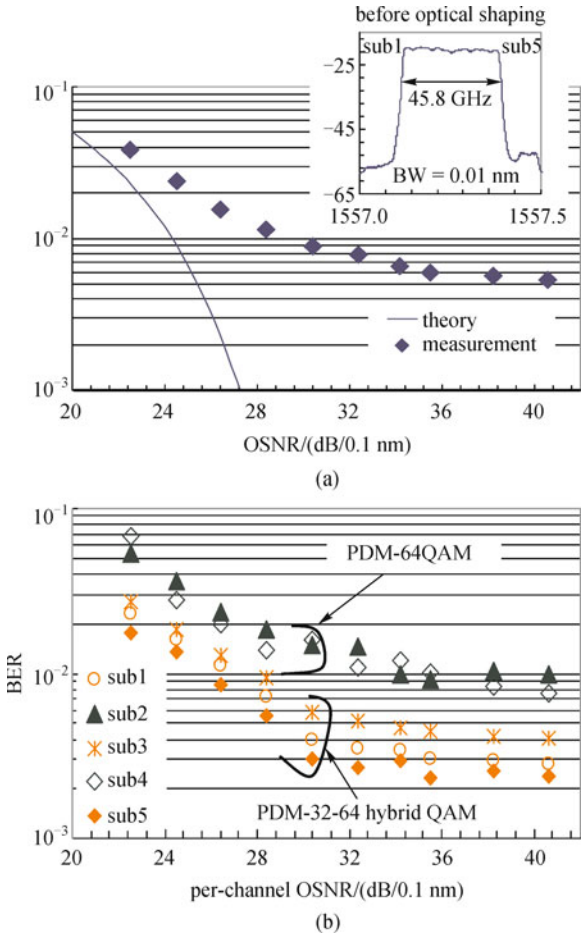

Fig. 13 Measured back-to-back BER performance versus the OSNR for single 504 Gb/s channel (before optical spectral shaping) (a) and for five individual subcarriers (b)

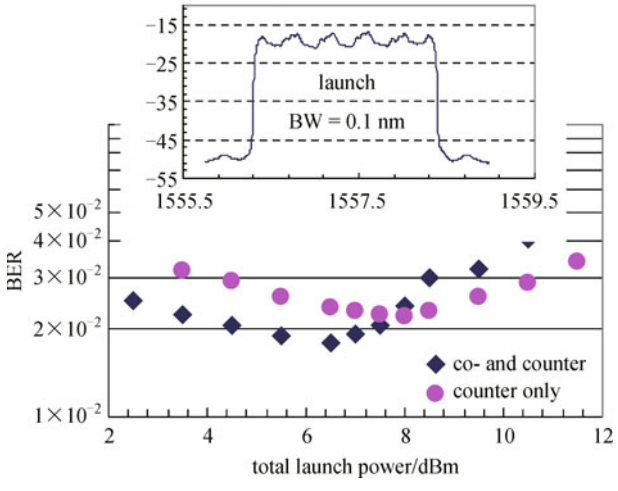

Fig. 14 Measured BER of center WDM channel vs. total launch power for two different amplification schemes, where the inset shows the measured optical spectrum of the five WDM channels launched into the ROADM

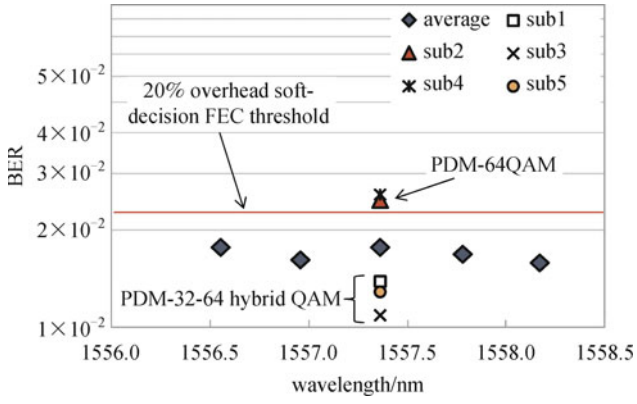

Fig. 15 BERs of all five 504 Gb/s WDM channels with co- and counter-pumped Raman

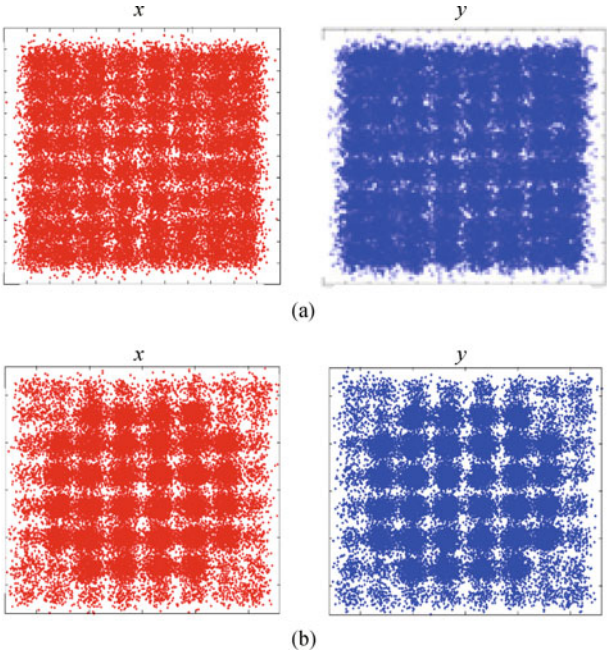

Fig. 16 Received constellation diagrams after 1200 km transmission for two subcarriers using different modulation formats. (a) Ch3, subcarrier 2, PDM-64QAM; (b) Ch3, subcarrier 5, PDM-32-64 hybrid QAM

representing 0.5 dB Q margin for 20% soft decision FEC using quasi-cyclic LDPC code with BER threshold 2.4×10^{-2} [34]. In this experiment, the use of more noise-tolerant time-domain hybrid QAM provided exactly the amount of extra SE to meet our FEC overhead requirement. Such a fine SE granularity requirement is impossible to realize when using a regular 2^m-ary QAM having a SE granularity of 1 b/s/Hz (2 b/s/Hz when using PDM). Because no inline optical dispersion was used. From the measured noise probability density function (PDF) of the recovered, we found that the noise statistics could be well approximated by an additive Gaussian distribution in both the linear and nonlinear regimes, agreeing with Ref. [35].

4 Discussion

In the two transmission experiments described above, state-of-the-art ULA fiber was used as the transmission fiber. Even with such a low-loss, large-effective-area fiber, the realized transmission reach is still not adequate for many long-haul transmission applications, and the transmission reach could be reduced by about 40% [36] when using deployed SSMFs. So significant efforts are needed to further extend the transmission reach. Although very challenging, there are still some possibilities for technologies that could be utilized to achieve this goal.

First, improved equalization and phase recovery algorithms could be used to reduce the implementation and transmission penalties. In the first described experiment using PDM-32QAM, we observed 3.2 dB back-to-back implementation penalty and an extra 4 dB transmission penalty. For the second experiment using PDM-32-64 hybrid QAM, we observed 2.5 dB back-to-back implementation penalty and close to 6 dB transmission penalty. Such large penalties could be reduced by combined use of three-stage cascaded equalization and training-assisted phase recovery [14]. The effectiveness of such improved equalization and phase recovery algorithms has been verified in our most recent 400 Gb/s point-to-point transmission experiment [14], where ten 50 GHz-spaced 494.5 Gb/s WDM signals were transmitted over more than 3000 km of ULAF by using PDM-32-64 hybrid QAM with back-to-back implementation penalty of less than 1.5 dB and transmission penalty of less than 2.5 dB. Second, we may still have >1 dB room to further improve FEC coding gain by joint optimization of the FEC code rate and modulation SE using time-domain hybrid QAM. Third, constellation shaping and/or optimization may be used to further improve the transmission performance. In our experiments, the standard 32QAM and 64QAM constellations that were used were not optimal in terms of both noise sensitivity and laser phase noise tolerance [37]. Fourth, better performance can be expected by using optimized all-Raman amplification. In our experimental system, the Raman amplifiers were not optimal because the forward Raman gain was too small. Optimized Raman amplification requires the development of high-power forward Raman pumps with low relative intensity noise and low degree of polarization. Although digital nonlinear compensation has received significant attention recently, for high-SE terrestrial systems using ROADMs to route wavelengths, backward-propagation-based nonlinear compensation may not be useful given its complexity and very limited performance improvement [38].

It is clear that more studies are needed to fully understand the feasibility of transmitting 400 Gb/s signals at 50 GHz channel spacing in realistic long-haul optical networks using SSMF as the transmission fiber. However, based on our experimental results, transmitting 400 Gb/s on the 50 GHz grid is promising for regional and

metropolitan optical networks where the typical transmission reach is below 600 km. By using only 50 GHz channel bandwidth for a 400 Gb/s signal, not only we can share more capacity over the common transport infrastructure (i.e., the fiber, amplifiers, and ROADMs), it also gives us the potential capability to modulate the 400 Gb/s signal on a single carrier using a single I/Q modulator and a single pair of A/D and D/A converters (within about five years a symbol rate between 40 and 45 Gb/s baud could be feasible). This may bring us significant cost advantages compared to the widely considered option for 400 Gb/s, which uses two subcarriers modulated with PDM-16QAM and comprises > 75 GHz channel bandwidth, because the use of two subcarriers require two sets of D/A and A/D converters and two modulators, including two high-speed electrical driving circuits.

Although only one ROADM was used in the two described 400 Gb/s transmission experiments, the very principle of using a broadband optical equalizer to precompensate the ROADM filtering effects just before the signal enters the ROADM has been demonstrated to be effective. Such an idea can be easily extended to a real system using multiple ROADMs along the transmission link by integrating an optical equalizer into each ROADM to perform distributed compensation of ROADM filtering.

Finally, it should be noted that, for some special cases where no ROADM is needed, i.e., point-to-point transmission, the transmission reach can be increased considerably by taking full use of the available 50 GHz channel bandwidth and the availability of SE-flexible modulation formats, as was demonstrated in Ref. [14], where a time-domain hybrid 32-64QAM with 5.1 bits/symbol SE has enabled 400 Gb/s WDM transmission over 32 × 100 km reach in 50 GHz channel spacing. This experiment also demonstrated that the use of two-stage equalization strategy with large second stage equalizer taps (along with training-assisted phase recovery following the first stage equalization) could effectively reduces the implementation penalty caused by some low-frequency or narrow-band distortion from imperfect D/A and A/D converters, as well as from the used non-ideal electro-optical modulators (see Fig. 17).

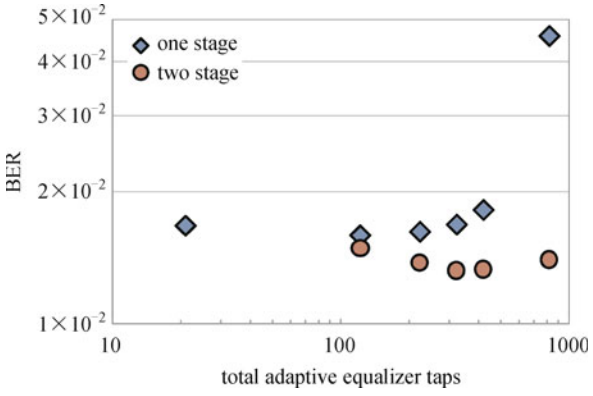

Fig. 17 Comparison between one-stage and two-stage equalization. For the two-stage case, Eq. (1) length was fixed at 21 taps while we increase the number of taps for Eq. (2)

5 Conclusions

This paper presents a compressive review of recent technology advancements related to 400 Gb/s WDM transmission with 50 GHz channel spacing, for future 50 GHz grid optical networks. It is shown that time-domain hybrid 32-64QAM, close to ideal digital Nyquist pulse shaping, distributed compensation of ROADM filtering, end-to-end carrier frequency control, distributed Raman amplification, and high-gain FEC coding (or coded modulation) are key enabling technologies. By using these technologies, five 400 Gb/s, 50 GHz-spaced WDM signals were successfully transmitted over 1200 km of ULAF and passed through one 50 GHz grid ROADM with −3 dB bandwidth 42.2 GHz. Without using ROADM, 400 Gb/s WDM transmission in 50 GHz channel spacing over more than 3000 km has also been demonstrated by using the proposed time-domain hybrid QAM technique, along with novel two-stage equalization and training-assited phase recovery algorithms.

Although the realized transmission reach is still not adequate for many long-haul optical networks, our transmission results do indicate that, for metropolitan and some regional applications, using the standard 50 GHz channel spacing for future 400 Gb/s systems could be a very attractive option. For those applications, 400 Gb/s on 50 GHz spacing may bring us significant cost advantages compared to the widely considered 400 Gb/s option using PDM-16QAM, two subcarriers and > 75 GHz channel bandwidth,

There is still room for us to further improve the transmission reach for a 50 GHz-spaced, 400 Gb/s system by reducing the implementation penalties through improved equalization and phase recovery algorithms, by joint optimization of modulation SE and FEC code rate, and by using an optimized constellation, as well as through improved Raman amplification schemes. It is clear that more study is needed to fully understand the feasibility and potential of 50 GHz-spaced 400 Gb/s systems to meet the requirements of realistic long-haul transmission applications.

References

1. Camera M, Olsson B E, Bruno G. Beyond 100 Gbit/s: System implications towards 400 G and 1 T. In: Proceedings of the 36th European Conference and Exhibition on Optical Communication 2010 Symposium toward 1 Tb/s. 2010, 1–28
2. Cole C. Is 1 Tb/s ready for prime time? Engineering reality check.

In: IEEE Photonics Society Summer Topical, Montreal, Canada, 2011. Terabit Optical Ethernet, WC1. 1

3. Yu J, Zhou X, Huang M-F, Qian D, Ji P N, Wang T, Magill P. 400 Gb/s (4 × 100 Gb/s) orthogonal PDM-RZ-QPSK DWDM signal transmission over 1040 km SMF-28. Optics Express, 2009, 20(17): 17928–17933
4. Liu X, Chandrasekhar S, Zhu B, Winzer P J, Gnauck A H, Peckham D W. Transmission of a 448-Gb/s reduced-guard-interval CO-OFDM signal with a 60-GHz optical bandwidth over 2000 km of ULAF and five 80-GHz-Grid ROADMs. In: Proceedings of conference on Optical Fiber Communication-National Fiber Optic Engineers Conference. 2010, PDPC2
5. Chandrasekhar S, Liu X, Zhu B, Peckham D W. Transmission of a 1.2-Tb/s 24-carrier no-guard-interval coherent OFDM superchannel over 7200-km of ultra-large-area fiber. In: Proceedings of the 35th European Conference on Optical Communication. 2009, PDP 2.6
6. Winzer P J, Gnauck A H, Chandrasekhar S, Draving S, Evangelista J, Zhu B. Generation and 1200-km transmission of 448-Gb/s ETDM 56-Gbaud PDM 16-QAM using a single I/Q modulator. In: Proceedings of 36th European Conference and Exhibition on Optical Communication. 2010, PDP 2.2
7. Gnauck A H, Winzer P J, Chandrasekhar S, Liu X, Zhu B, Peckham D W. 10 × 224-Gb/s WDM transmission of 28-Gbaud PDM 16-QAM on a 50-GHz grid over 1200 km of fiber. In: Proceedings of conference on Optical Fiber Communication-National Fiber Optic Engineers Conference. 2010, PDPB8
8. Huang Y K, Ip E, Huang M, Zhu B, Ji P N, Shao Y, Peckham D W, Lingle R , Aono Y, Tajima T, Wang T. 10×456 Gb/s DP-16QAM Transmission over 8×100 km of ULAF using Coherent Detection with a 30-GHz Analog-to-Digital Converter. In: Proceedings of the 15th OptoeElectronics and Communications Conference. 2010, PDP3
9. Takahashi H, Takeshima K, Morita I, Tanaka H. 400-Gbit/s Optical OFDM Transmission over 80 km in 50-GHz Frequency Grid. In: Proceedings of European Conference on Optical Communication. 2010, Tu.3.C.1
10. Zhou X, Nelson L E, Magill P, Isaac R, Zhu B, Peckham D W, Borel P, Carlson K. 8×450 Gb/s, 50 GHz-spaced, PDM-32QAM transmission over 400 km and one 50 GHz-grid ROADM. In: Proceedings of conference on Optical Fiber Communication-National Fiber Optic Engineers Conference. 2011, PDPB3
11. Zhou X, Nelson L, Magill P, Isaac R, Zhu B, Peckham D W, Borel P, Carlson K. 800 km transmission of 5×450 Gb/s PDM-32QAM on the 50 GHz grid using electrical and optical spectral shaping. In: Proceedings of European Conference and Exposition on Optical Communications. 2011, We.8.B.2
12. Zhou X, Nelson L E, Magill P, Isaac R, Zhu B, Peckham D W, Borel P, Carlson K. 1200 km Transmission of 50 GHz spaced, 5×504 Gb/s PDM-32-64 hybrid QAM using Electrical and Optical Spectral Shaping. In: Proceedings of conference on Optical Fiber Communication-National Fiber Optic Engineers Conference. 2012, OM2A.2
13. Kobayashi T, Sano A, Matsuura A, Miyamoto Y, Ishihara K. Nonlinear tolerant long-haul WDM transmission over 1200 km using 538 Gb/s/ch PDM-64QAM SC-FDM signals with pilot tone. In: Proceedings of conference on Optical Fiber Communication-National Fiber Optic Engineers Conference. 2012, OM2A.5
14. Zhou X, Nelson L E, Magill P, Isaac R, Zhu B, Peckham D W, Borel P, Carlson K. High spectral efficiency 400 Gb/s transmission using PDM time-domain hybrid 32-64QAM and training-assisted carrier recovery. Journal of Lightwave Technology, Feburary issue of 2013
15. Proakis J G. Digital Communication. 4rd ed. NY: McGraw-Hill, 2001
16. Zhou X, Yu J. Multi-level, multi-dimensional coding for high-speed and high spectral-efficiency optical transmission. Journal of Lightwave Technology, 2009, 27(16): 3641–3653
17. Pfau T, Hoffmann S, Noé R. Hardware-efficient coherent digital receiver concept with feed-forward carrier recovery for M-QAM constellations. Journal of Lightwave Technology, 2009, 27(8): 989–999
18. Zhou X, Yu J, Huang M F, Shao Y, Wang T, Nelson L, Magill P, Birk M, Borel P I, Peckham D W, Lingle R, Zhu B. 64 Tb/s, 8 b/s/Hz, PDM-36QAM transmission over 320 km using both pre- and post-transmission digital signal processing. Journal of Lightwave Technology, 2011, 29(4): 571–577
19. Peng W R, Morita I, Tanaka H. Hybrid QAM transmission techniques for single-carrier ultra-dense WDM systems. In: Proceedings of the 16th OptoeElectronics and Communications Conference. 2011, 824–825
20. Takahashi H, Morita I, Tanaka H. The impact of the combined 8-QAM and QPSK subcarrier modulation for coherent optical OFDM. In: Proceedings of conference on Optical Fiber Communication-National Fiber Optic Engineers Conference. 2011, JWA30
21. Schmogrow R, Winter M, Meyer M, Hillerkuss D, Wolf S, Baeuerle B, Ludwig A, Nebendahl B, Ben-Ezra S, Meyer J, Dreschmann M, Huebner M, Becker J, Koos C, Freude W, Leuthold J. Real-time Nyquist pulse generation beyond 100 Gbit/s and its relation to OFDM. Optics Express, 2012,1(20): 317–337
22. Nelson L E, Woodward S L, Foo S, Moyer M, Yao D, O'Sullivan M. 100 Gb/s dual-carrier DP-QPSK performance after WDM transmission including 50 GHz wavelength selective switches. In: Proceedings of conference on Optical Fiber Communication-National Fiber Optic Engineers Conference. 2011, NWA2
23. Zhou X, Nelson L E, Magill P, Isaac R, Zhu B, Peckham D W, Borel P, Carlson K. PDM-Nyquist-32QAM for 450-Gb/s per-channel WDM transmission on the 50 GHz ITU-T grid. Journal of Lightwave Technology, 2012, 30(4): 553–559
24. OIF-ITLA-MSA-01.1, Optical Internetworking Forum, 2005, 91
25. Chang F, Onohara K, Mizuochi T. Forward error correction for 100 G transport networks. IEEE Communications Magazine, 2010, 48 (3): S48–S55
26. Nelson L E, Pan Y, Birk M, Isaac R, Rasmussen C, Givehchi M, Mikkelsen B. WDM performance and multiple-path interference tolerance of a real-time 120 Gbps pol-mux QPSK transceiver with soft decision FEC. In: Proceedings of conference on Optical Fiber Communication-National Fiber Optic Engineers Conference. 2012, NTh1I.5
27. Chang D, Yu F, Xiao Z, Stojanovic N, Hauske F N, Cai Y, Xie C , Li L, Xu X, Xiong Q. LDPC convolutional codes using layered decoding algorithm for high speed coherent optical transmission. In: Proceedings of conference on Optical Fiber Communication-

National Fiber Optic Engineers Conference. 2012, OW1H.4

28. Cai Y. Limit on coding and modulation gains in fiber-optic communication systems. In: Proceedings of Wireless and Optical Communications Conference. 2005, F9
29. Zhang G, Nelson L E, Pan Y, Birk M, Skolnick C, Rasmussen C, Givehchi M, Mikkelsen B, Scherer T, Downs T, Keil W. 3760 km, 100 G SSMF transmission over commercial terrestrial DWDM ROADM systems using SD-FEC. In: Proceedings of conference on Optical Fiber Communication-National Fiber Optic Engineers Conference. 2012, PDP5D.4
30. Zhou X, Birk M. New design method for a WDM system employing broad-band raman amplification. IEEE Photonics Technology Letters, 2004, 16(3): 912–914
31. Zhou X, Yu J, Huang M F, Shao Y, Wang T, Nelson L E, Magill P D, Birk M, Borel P I, Peckham D W, Lingle R, Zhu B. 64-Tb/s, 8 b/s/Hz, PDM-36QAM transmission over 320 km using both pre- and post-transmission digital signal processing. Journal of Lightwave Technology, 2011, 29(4): 571–577
32. Fang T T. Analysis of self-noise in a fourth-power clock regenerator. IEEE Transactions on Communications, 1991, 39(1): 133–140
33. Zhou X. An improved feed-forward carrier recovery algorithm for coherent receiver with M-QAM modulation format. IEEE Photonics Technology Letters, 2010, 22(14): 1051–1053
34. Chang D, Yu F, Xiao Z, Stojanovic N, Hauske F N, Cai Y, Xie C. FPGA verification of a single QC-LDPC code for 100 Gb/s optical systems without error floor down to BER of 10^{15}. In: Proceedings of conference on Optical Fiber Communication-National Fiber Optic Engineers Conference. 2011, OTuN2
35. Vacondio F, Simonneau C, Lorcy L, Antona1 J C, Bononi A, Bigo S. Experimental characterization of Gaussian-distributed nonlinear distortions. In: Proceedings of European Conference and Exposition Optical Communications. 2011, We.7.B.1
36. Zhu B, Chandrasekhar S, Liu X, Peckham D W. Transmission performance of a 485-Gb/s CO-OFDM superchannel with PDM-16QAM subcarriers over ULAF and SSMF-based links. IEEE Photonics Technology Letters, 2011, 23(19): 1400–1402
37. Dischler R. Experimental comparison of 32- and 64-QAM constellation shapes on a coherent PDM burst mode capable system. In: Proceedings of the 37th European Conference Exhibition on Optical Communication. 2011, Mo. 2.A.6
38. Mateo EF, Zhou X, Li G. Selective post-compensation of nonlinear impairments in polarization-division multiplexed WDM systems with different channel granularities. IEEE Journal of Quantum Electronics, 2011, 47(1): 109–116